

Tribology in Warm and Hot Aluminum Sheet Forming: Transferability of Strip Drawing Tests to Forming Trials


Lukas Schell,* Erik Sellner, Michael Massold, and Peter Groche

For conventional sheet metal forming at room temperature, numerous tribometers have been developed in the 20th century. At the present state of the art, there are some challenges for tribometry in warm and hot forming processes of high-strength aluminum (e.g., EN AW-7075). Especially for nonisothermal processes with heated sheets and cooled dies, the tribological design is a major challenge, which needs to be addressed by investigations with adapted tribometers. Herein, the transferability of friction and wear behavior of three different lubricants and temperatures is investigated. Therefore, tribometer test results are compared with real forming trials in combination with thermomechanical finite element simulations. Both the behavior of different lubricant types and the characteristics of tool lubrication in sheet metal forming are discussed.

1. Introduction

High-strength aluminum sheets (e.g., EN AW-7075) hold great potential in lightweight applications, but have low formability at room temperature.^[1] For this reason, several temperature-supported process routes are being investigated.^[2] In warm and hot aluminum sheet metal forming processes, the sheets are preheated to temperatures between approximately 200 and 550 °C, depending on the alloy and the process route. Forming at elevated temperatures represents a high thermal load for the tribological system and prevents a wide application of warm and hot forming of aluminum sheets in series production.^[3] Lubrication of cold tools, instead of sheet lubrication, reduces the thermal load on the lubricant^[4] and is therefore used by several researchers and companies around the world.^[1,2,4–7] Both the elevated sheet temperatures and the concept of tool lubrication need to be considered in tribological investigations of high-strength aluminum forming.

L. Schell, E. Sellner, M. Massold, P. Groche
Institute for Production Engineering and Forming Machines
Technical University of Darmstadt
Otto-Berndt-Str. 2, 64287 Darmstadt, Germany
E-mail: schell@ptu.tu-darmstadt.de

 The ORCID identification number(s) for the author(s) of this article can be found under <https://doi.org/10.1002/adem.202201900>.

© 2023 The Authors. Advanced Engineering Materials published by Wiley-VCH GmbH. This is an open access article under the terms of the Creative Commons Attribution-NonCommercial License, which permits use, distribution and reproduction in any medium, provided the original work is properly cited and is not used for commercial purposes.

DOI: 10.1002/adem.202201900

For conventional room temperature sheet metal forming, several dedicated tribometers have already been developed. An overview of these tribometers can be found in recent literature.^[8,9] The tribometers for investigating warm and hot sheet metal forming can be classified in two categories: oscillating tribometers and strip drawing tests. Investigations on oscillating tribometers are mainly limited to dry condition^[10] or the use of long-term temperature-stable lubricants like boron nitride,^[11] boron nitride and graphite^[12,13] or a combination of both.^[14] The reason for this limitation is the long duration of oscillating experiments, which results in an unrealistically long temperature exposure of the

lubricant compared to nonisothermal forming processes with tool lubrication. When using other lubricants in oscillating tribometer tests, e.g., silicon polymer,^[15] the test temperatures have been slightly reduced from hot forming temperatures (>400 °C) to 300 °C. In isothermal strip drawing tests, similar approaches are used: either the temperature is lower than hot forming temperature^[16] or high-temperature lubricants, e.g., MoS₂, graphite^[17] or boron nitride,^[18] are used. In the nonisothermal strip drawing tests of Liu et al., the dies were clamped onto the cold part of the strip before the drawing process started. The first two seconds of sliding at 50 mm s⁻¹ are between lubricated dies and cold aluminum strip, before the hot part of the strip enters the sliding zone.^[19] This test procedure might scrape the lubricant from the dies or at least change the lubricant's structure. In tempered strip drawing tests of Rigas et al., a dry lubricant is applied to the aluminum strip and a single-sided die with a contact area of 16 mm² is used.^[20] This configuration resembles a pin on disc test with an open tribological system.

An adapted strip drawing test for warm and hot forming processes has already been presented by the authors.^[21] A comprehensive study of several lubricant classes at various temperatures in the strip drawing test demonstrated differences in coefficient of friction (COF) and wear performance.^[22] In the present article, the transferability of these results to a real forming process of a hat geometry is investigated.

2. Experimental Section

Figure 1 shows the general approach of the present article. The experimental and finite element (FE) analysis setups are described in the following sections.

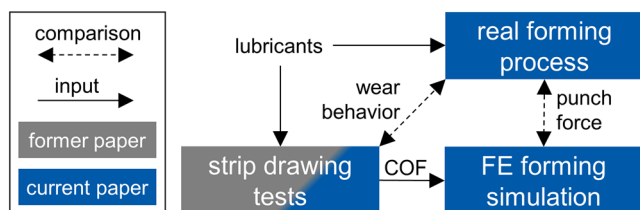


Figure 1. Schematic approach and context of the current investigation (COF = coefficient(s) of friction; FE = finite element).

2.1. Experimental Investigation

2.1.1. General Information and Lubrication

The experimental investigations were performed with 1.5 mm-thick sheet material EN AW-7075 T6 (AMAG Austria Metall AG) in combination with hot work tool steel Uddeholm Unimax (57 HRC).

In both the strip drawing tests and the forming trials, the concept of tool lubrication was used with the lubricants summarized in **Table 1**. These lubricants were selected based on discussions with lubricant manufacturers and market research. One objective was to test lubricants from different classes to account for different lubricant-specific effects. It should be noted that the lubricants were not developed specifically for this application. Therefore, no general statement can be made about the overall quality of the lubricant. The dies of the strip drawing test were lubricated with a spray gun. The amount of lubricant was controlled gravimetrically with a metal test sheet that was simultaneously lubricated (oil $\approx 7 \text{ g m}^{-2}$, polymer $\approx 16 \text{ g m}^{-2}$, BN $\approx 24 \text{ g m}^{-2}$). The lubricant quantities were chosen to ensure a minimum COF for the specific lubricant, with higher lubricant quantities having no additional positive effect.^[22] Due to limited accessibility, the forming tools were lubricated with a roller, approximating a similar amount of lubricant. Application was performed at room temperature, and the polymer and the BN were dried with a hot air gun at temperatures below 100 °C prior to testing. The tests were performed with dies and lubricant at room temperature, approximately 5–20 min after lubrication. Although this method of application may differ from the methods intended by the manufacturers (e.g., billet coating), to the best of our knowledge, after consultation with the manufacturers, it does not affect the performance of the lubricant.^[22]

2.1.2. Strip Drawing Tests

The core components of the tempered strip drawing test are heating plates with heating cartridges to heat up the aluminum strip

(up to 550 °C). The dies are temperature controlled from 20 to 450 °C with heating cartridges in their base plate in combination with water cooling channels.^[21] The COF values used in this article were determined in a previous publication in flat die strip drawing tests. The initial strip temperatures were 425 °C (hot), 225 °C (warm), and room temperature (RT) at the start of the drawing process. The contact area was $55 \times 130 \text{ mm}^2$ with polished dies ($R_z = 0.44 \mu\text{m} \pm 0.15 \mu\text{m}$). The drawing speed was 100 mm s^{-1} , the drawing length was 130 mm, and the contact pressure was 3, 5, and 20 MPa, respectively. For each parameter combination, three tests were performed, and the COF was averaged separately before and after the onset of adhesive wear. The onset of wear was determined visually. The wear-free draw-in was measured from the wear marks on the aluminum strips.^[22]

2.1.3. Forming Trials

In the forming trials, blanks with the dimensions $70 \times 230 \times 1.5 \text{ mm}^3$ were formed to an open hat profile in a multipurpose forming tool (**Figure 2a,b**). The active tool parts are made of the hot work tool steel Uddeholm Unimax and the die radii are polished initially to a roughness of $R_z = 0.687 \mu\text{m} \pm 0.20 \mu\text{m}$ measured with a μSurf confocal microscope from nanofocus in combination with a Struers RepliSet. Over the course of the tests, roughness changed slightly to a maximum of $R_z = 1.21 \mu\text{m} \pm 0.10 \mu\text{m}$, due to wear removal with a radial bristle Disc K220 from 3M. The change in roughness did not change the forming results (punch force, wear behavior). Prior to forming, the blanks were heated in a Nabertherm NA 15/65 forced convection chamber furnace to 245 and 350 °C, respectively. The forming tool is at room temperature. To avoid excessive precooling of the blank, it was placed on spring-loaded pins 5 mm above the blank holder surface. The forming trials were carried out on a Synchropress SWP 2500 with the schematic tool and the press stroke shown in **Figure 2c,d**. The blank holder distance is set to 2 mm in the steps II–IV resulting in a gap of 0.5 mm between blank and die/blank holder in the flange area. During the forming process (III), the punch force was measured with two MecSense C2S load cells. Additional evaluation variables are the roughness of the formed parts, measured with a Hommel T800 with a $2 \mu\text{m}$ 90° probe tip to quantify wear.

It should be noted that there is a difference in sheet temperature between the hot strip drawing tests (425 °C) and the hot forming trials (325 °C). The difference is due to the fact that the aluminum blanks cracked during the forming process when

Table 1. Tested lubricants with primary use cases and properties as specified by the manufacturers.

Shortcut	Lubricant name and properties	Primary use case
Oil	MKU Putrol NW V 1933–30 N-1 mineral oil with additives, kin. viscosity (40 °C) = $530 \text{ mm}^2 \text{ s}^{-1}$	Special drawing oil for aluminum and copper alloys; continuous casting using the airslip process; mold release agent for continuous casting
Polymer	ZWEZ-Lube PD 5942 (test product)	Billet coating for bulk metal forming
BN	H.C. Carbon Mechano Lube 6VP813 (6D1 for strip drawing at RT)	Metal forming (esp. die forging) and aluminum casting; billet coating; stable till $>1000 \text{ °C}$

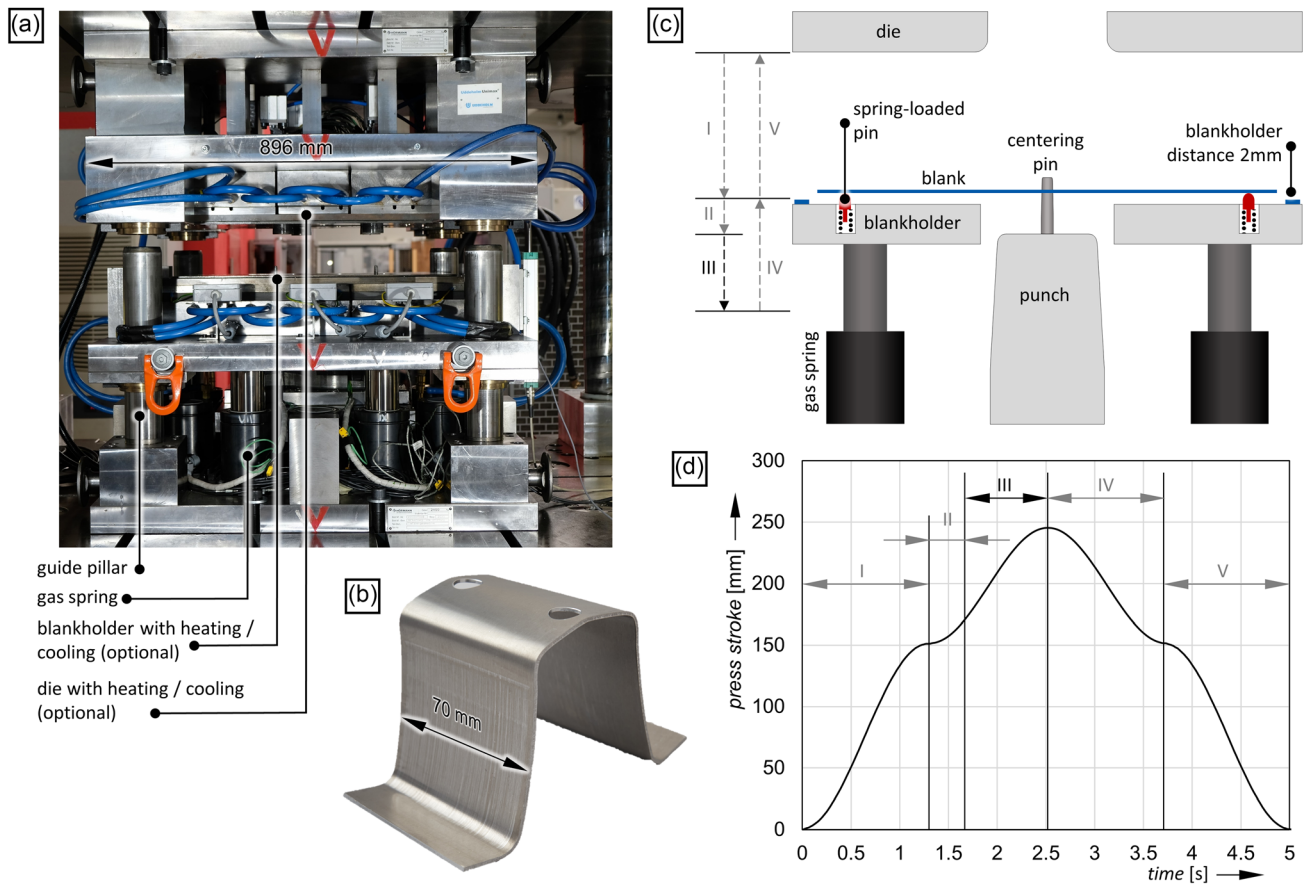


Figure 2. a) Multipurpose forming tool as photo, b) formed part, c) forming tool as schematic, d) press stroke in the forming trials with (I) die closure, (II) idle stroke, (III) forming (75 mm), (IV) return stroke, and (V) die opening.

the furnace temperature was set above 350 °C. This occurred due to excessive restraining forces despite a distanced blank holder. To account for the temperature deviation, the COF from the strip drawing tests at both 225 and 425 °C is considered when comparing the experimental and FE results at the hot forming temperature (Section 3.3.3).

2.2. FE Analysis

The FE model was set up as a thermomechanical quarter model in Abaqus 6.14-1 (cf., **Figure 3a,b**).

The plastic behavior of the blank was modeled using temperature-dependent flow curves (200, 250, 300, 350, and 400 °C)

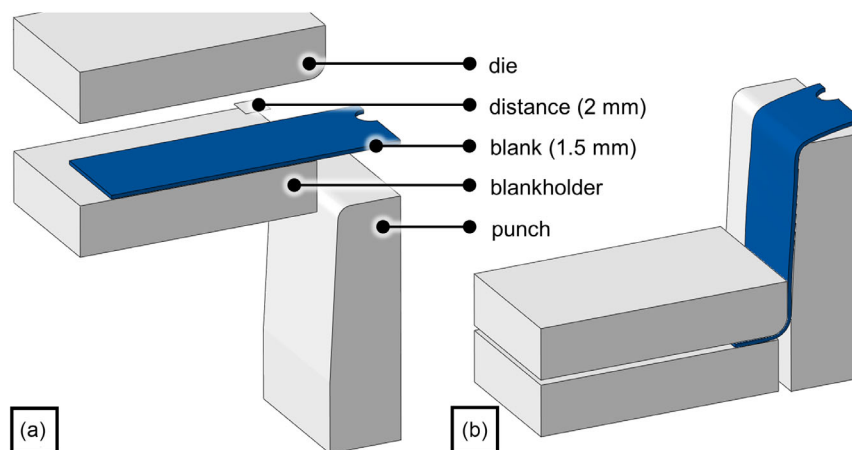


Figure 3. a) FE model of the forming process in the initial state and b) at the end of the forming process.

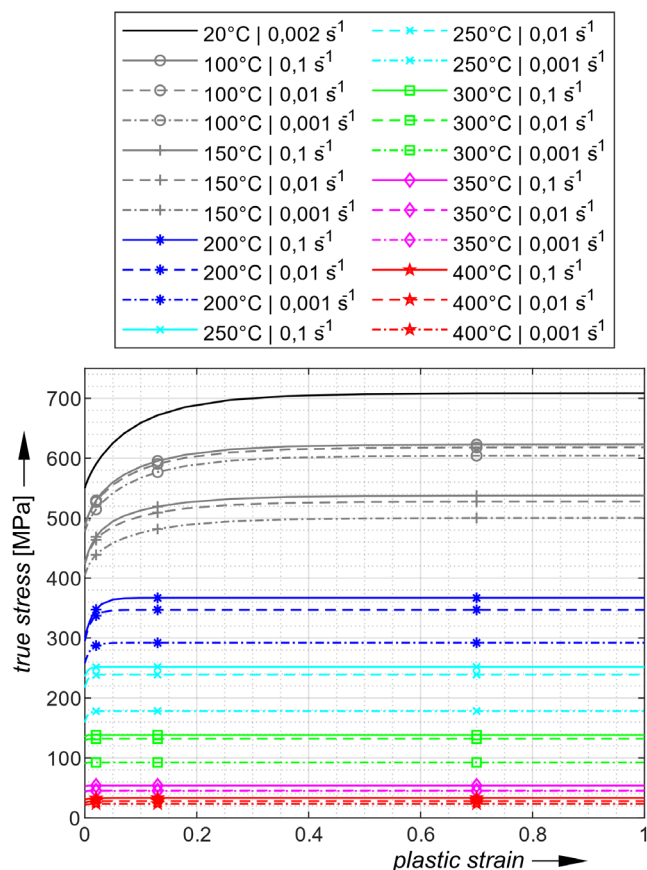


Figure 4. Temperature-dependent flow curves of EN AW-7075, including synthetic flow curves for 100 and 150 °C.

based on the tensile test data from Sajadifar et al.^[23] In addition, a flow curve from the same material batch at 20 °C was determined by the authors. All experimental flow curves were obtained using a Hocket–Sherby approach and are plotted in **Figure 4**. The flow stress between the experimental flow curves at the specified temperatures is linearly interpolated, with one exception: tensile tests from the literature indicate a nonlinear increase in (engineering) stress between 200 and 20 °C.^[24] To account for this material behavior, synthetic flow curves for 150 and 100 °C were added. The 150 °C flow curves are in the middle of the corresponding 200 and the 20 °C flow curves. The 100 °C flow curves are midway

Table 2. Modeling parameters for the FE analyses.

Thermal conductivity (20–500 °C)	Unimax dies: 27–29 W m ⁻¹ K ⁻¹ , cf., [34] 7075 sheet: 121–158 W m ⁻¹ K ⁻¹ , cf., [35]	Specific heat (30–500 °C)	Unimax dies: 460–656 J kg ⁻¹ K ⁻¹ , cf., [34,36] 7075 sheet: 863–1102 J kg ⁻¹ K ⁻¹ , cf., [35]
Contact behavior	Exponentially softened kinematic $p(5\ \mu\text{m}) = 0\ \text{MPa}$ $p(0\ \mu\text{m}) = 3\ \text{MPa}$ contact damping 0.1	COF	Constant; 0.01, 0.1, 0.2, 0.3, 0.4
Elements	C3D8T blank: 0.75 × 0.75 × 0.5 mm ³ ($l \times w \times h$) die radius: 0.5 × 2 × 0.5 mm ³ ($l \times w \times h$)	Solver	Explicit

between the 150 and 20 °C flow curves. The resulting nonlinear interpolation between the 20 and 200 °C flow curves is similar to the flow curves found in the literature for this temperature range.^[25,26]

Both sheet and tool temperatures are set to a homogeneous predefined temperature field at the beginning of the simulation. Heat transfer between the sheet and the tool is modeled using a pressure-dependent IHTC curve from Liu et al.^[27] The tool movement in the FE forming step was approximated to the experimental motion curve from Figure 2d, zones II and III. To reduce the simulation time, the blank holder closure (zone I) was shortened to 0.01 s and the initial temperature at the beginning of the forming step was approximated to experimentally measured data over the forming process. In addition, mass scaling by a factor of 1000 was used and other modeling parameters are shown in **Table 2**. The various COFs were each kept constant for the entire model. A convergence analysis led to the specified element size. A contact damping of 0.1 reduces the solution noise without affecting the punch force level, which was ensured in a comparative study. As in the experimental study, the punch force is the main evaluation variable in the FE analyses. It was determined from the reaction force of the rigid body punch, scaled from the symmetrical quarter model to the full model.

3. Results and Discussion

Section 3.1 provides an overview of the temperature- and lubricant-dependent experimental results. The results of the FE analyses are then presented in Section 3.2. Section 3.3 correlates the experimental and FE results and discusses the transferability for each temperature–lubricant combination.

3.1. Experimental Results

The COF results from the strip drawing test in **Figure 5** represent mean values from both wear-free sliding and sliding after the onset of wear. Most of the values are taken from the authors' previous investigation, which includes a further discussion of the strip drawing test results.^[22] A general trend is an increase in COF with initial sheet temperature and also after the onset of wear. An exception is the polymer lubricant, whose COF decreases with increasing temperature due to softening effects in the polymer that reduce its internal friction.^[22] During a single strip drawing test, the mean temperature in the friction zone

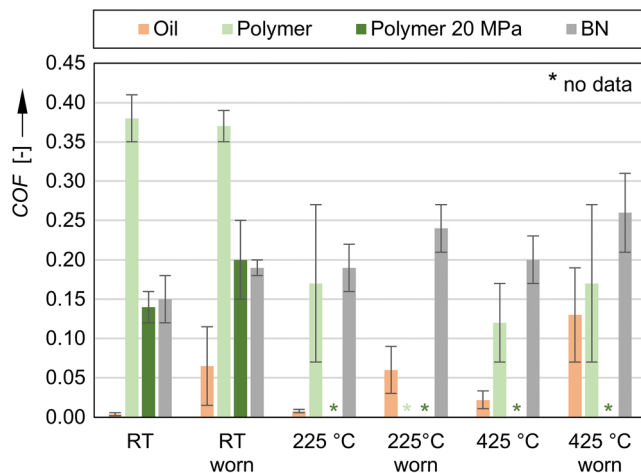


Figure 5. COF from the strip drawing test with tool lubrication at 5 MPa (RT and warm) and 3 MPa (hot), values extracted from a previous publication.^[22] COF values for polymer at 20 MPa were determined separately in the current contribution.

increases due to the draw-in of hot aluminum strips.^[21] A similar behavior, although in a weakened form, is expected for the polymer RT strip drawing test at 20 MPa due to frictional heat. In the case of the polymer lubricant, the decrease in COF with temperature and the increase in COF with wear partially offset each other.

Figure 6 shows the roughness values R_z and R_z max of the formed parts in the wall area that slid over the die radius during forming. Images of this area are shown in **Figure 7**. In the following, the results for polymer and BN are discussed first, followed by those for oil. For the polymer and the BN, surface roughness increases with increasing temperature due to increased galling of the aluminum on the die radius. This galling damages the blank surface especially at high temperatures, where scratches are visible from the beginning of the sliding

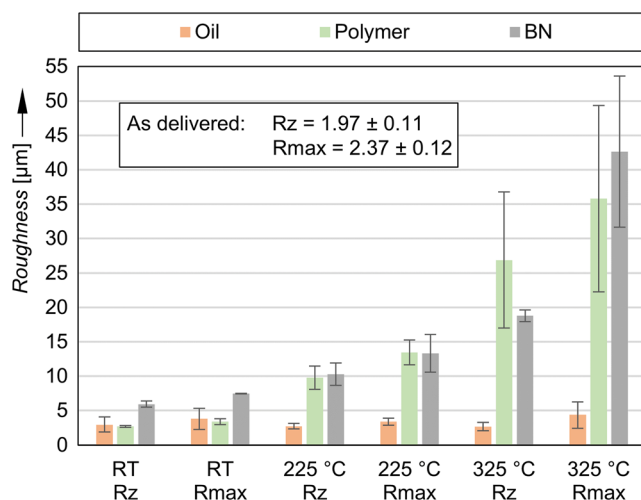


Figure 6. Surface roughness at the wall of the formed specimen and the blanks as delivered.

contact between the blank and the die radius. For BN, individual scratches with large undamaged areas (warm) or narrow undamaged streaks (hot) are visible at elevated temperatures. This behavior is consistent with previous results from the strip drawing test, which showed local stochastic detachment of BN from the die surface along with large areas of intact lubricant layers after pressure and sliding load.^[22] The polymer shows a more homogeneous wear distribution than the BN. It also exhibits a later onset of wear after a sliding distance of 11 mm (warm) or 10 mm (hot), which can be assumed to be the distance after which the lubricant is scraped off the die radius and direct aluminum–steel contact is initiated (cf., Figure 7). The BN and the polymer forming trials show more galling and scratches on the aluminum parts, and therefore poorer wear resistance, compared to the strip drawing tests with the same lubricants. This can be explained by the different contact conditions in the flat die strip drawing test compared to the die radius of sheet metal forming processes.^[28]

The oil lubricant shows a better wear reduction behavior with less galling and scratches on the formed aluminum parts, compared to the BN. For the oil, only minor changes in surface roughness were observed at all temperatures (cf., Figure 6), which is also indicated by the visual assessment in Figure 7. This behavior is surprising at first glance because the oil showed rather poor wear reduction behavior in the strip drawing tests at high temperatures.^[22] One explanation for the good wear behavior of the oil during forming is the transfer of oil from the die to the blank prior to the sliding process: At the end of step I (Figure 2c,d), the flange area of the blank is in contact with the lubricated die surface due to the spring-loaded pins (cf., **Figure 8**). Due to its liquid form, the oil transfers to the blank and thus prelubricated aluminum slides over the die radius, whereas in the strip drawing test, a dry aluminum strip enters the sliding zone. On the other hand, the BN and the polymer do not transfer from the flat die area to the blank in step I because of the solid form of the lubricants and the very low contact pressure between the flat die area and the blank (the contact pressure is only caused by the spring-loaded pins, cf., Figure 8a). This behavior was validated by inserting a blank and closing the die until just before the forming begins (end of step 2 in Figure 2), with no visible transfer of BN or polymer to the blank. As the blank holder distance is 0.5 mm greater than the blank thickness, there is no significant blank–die contact in the flat die area during the forming process, as seen in the FE forming simulation cross sections in Figure 8b. As an additional validation, it was observed after forming that both the polymer and the BN layer were still intact in the flat die area, while they were scraped from the die radius and to some extent from the blank holder contact area. For the polymer, the removal of lubricant at the die radius and subsequent dry aluminum contact results in wear marks on the formed parts after 10 and 11 mm, respectively (cf., Figure 7).

In summary, different lubricants have individual friction and wear characteristics in the current forming process. It was shown that the performance of a lubricant may depend on its ability to transfer from the die to the blank at low contact pressure. If lubricant transfer from die to blank is achieved immediately prior to the forming/sliding process (e.g., by low pressure contact between blank and die), dry aluminum sliding and thus galling can be significantly reduced.

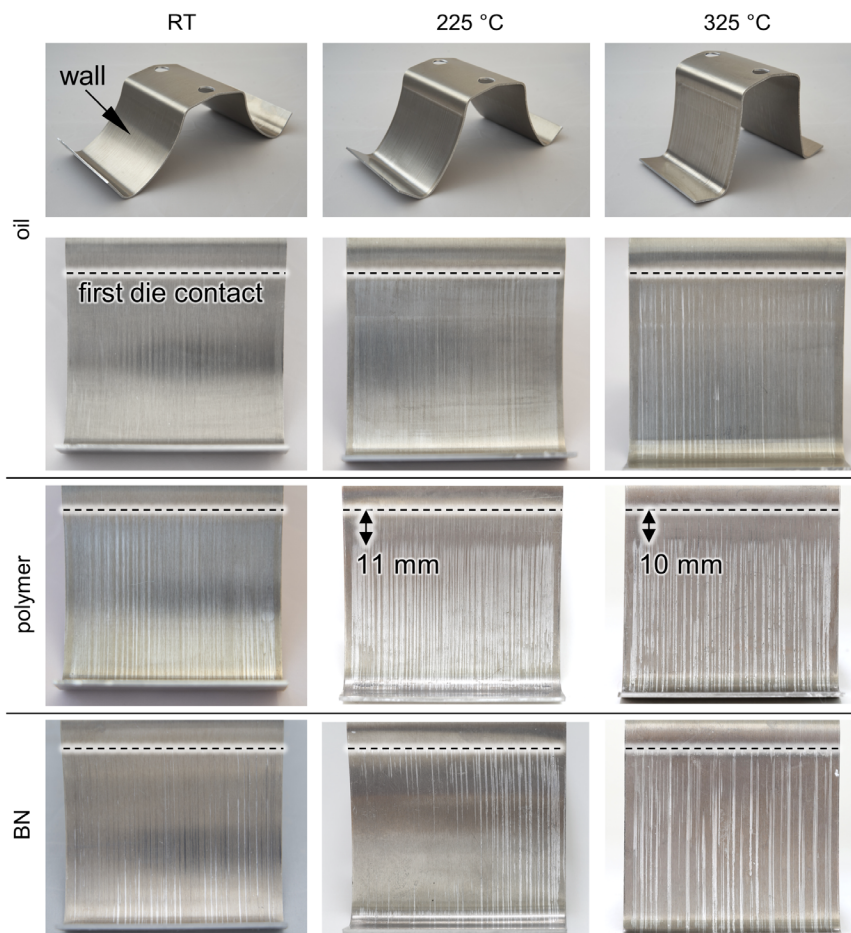


Figure 7. Geometry and surface quality at the wall area of the formed parts.

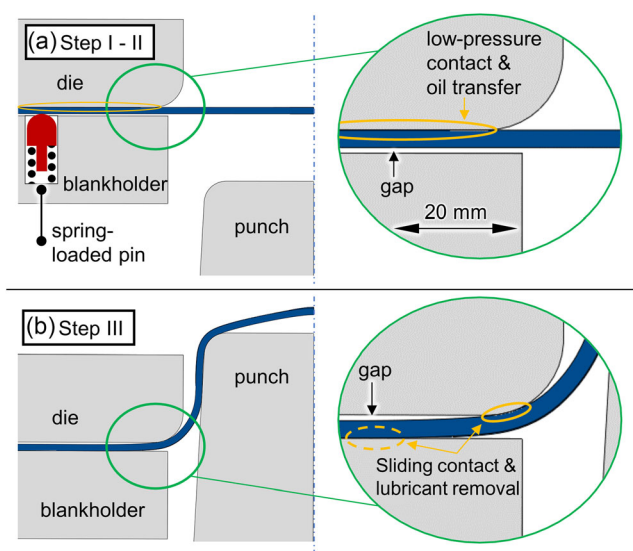


Figure 8. a) Blank–die contact after die closure and b) during forming. Blue and gray cross sections are taken from the FE analysis.

3.2. FE Results

The FE-based punch force curves over the time of the forming step are shown in **Figure 9** for different forming temperatures and COF. As expected, increasing the COF leads to higher restraining forces at the die radius and thus to higher punch forces. In absolute values, for RT, the COF-induced punch force increase is approximately 11.6 kN at 0.4 s. For warm forming it is 7.9 kN and for hot forming it is 6.2 kN. The reason for this variation in punch force increase is the temperature-induced reduction of the aluminum yield stress, which, in turn, reduces the contact pressure and thus the frictional component of the punch force. The increase in punch force over time (read: over press stroke) can be explained by an increasing bend angle at the die radius and thus an increasing amount of forming work. At elevated forming temperatures, part of the increase in punch force over time is due to the cooling of the sheet during the process, which increases the yield stress of the aluminum.

The jump of the punch force at about 0.2 s at low COFs (especially 0.01) is due to the sudden contact of the aluminum blank with the punch wall, which changes the kinematics of the forming process. At higher COFs (e.g., 0.4), the contact is initiated more smoothly due to a higher frictional restraining force that straightens the wall of the aluminum part (cf., **Figure 10**).

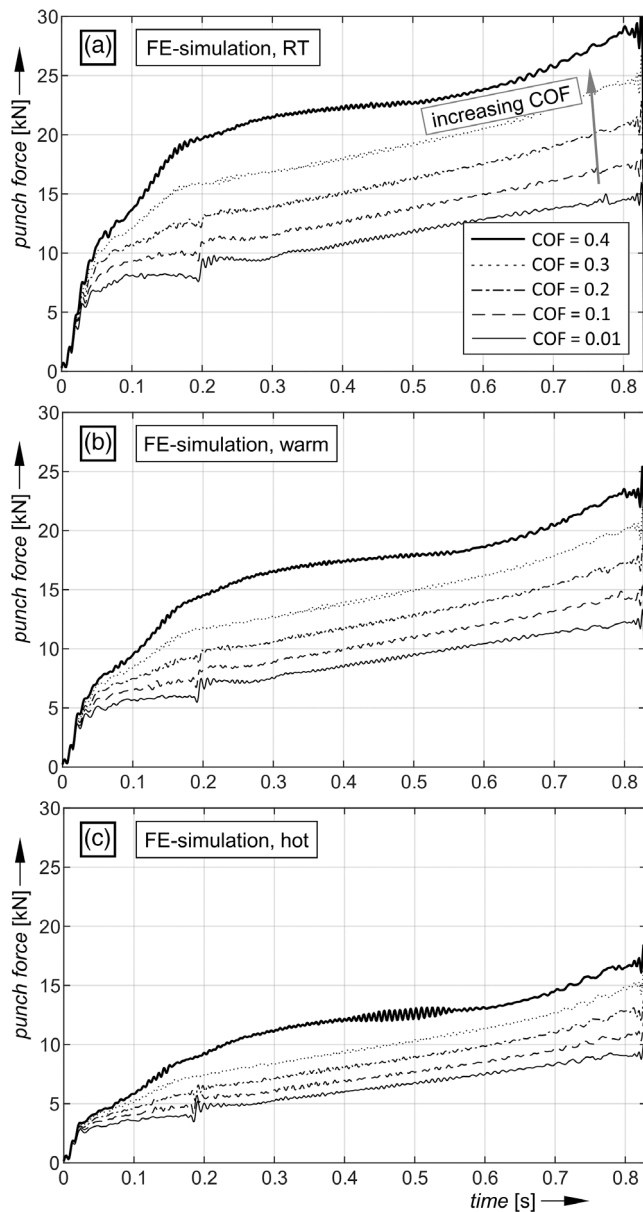


Figure 9. FE punch forces from different COFs and initial sheet temperatures: a) RT, b) warm, and c) hot.

Overall, the FE results are consistent with expectations based on basic knowledge of temperature-dependent material data and frictional behavior associated with sheet metal forming processes.

3.3. Transferability between Experimental and FE Results

In the following sections, the transferability of the results from the strip drawing tests (COFs, cf., Figure 5) to real forming processes is discussed. Therefore, experimental punch forces from different lubricants are compared with FE punch forces from different COFs. The comparison is structured by temperature and will be discussed in the following sections. The highlighted punch force curves in Figure 11–18 indicate the lubricant-

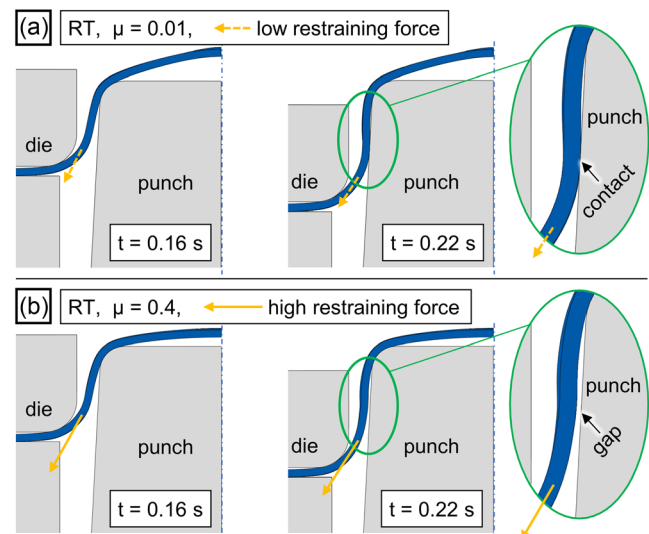


Figure 10. Aluminum to punch contact in the FE simulation at RT for a) low and b) high COFs.

specific COF expected from the strip drawing test for the FE analyses. For the experimental punch forces, the average of three experiments is plotted along with a shaded slope marking the maximum and minimum experimental punch forces at each measurement point.

3.3.1. RT Forming

The experimental and FE results for the oil lubricant at RT are shown in Figure 11 and show excellent agreement. The experimental force plotted after ≈ 0.83 s is from the return stroke, which was not simulated in the FE model. It can be concluded that for the oil, the COF from the strip drawing test can be transferred to the FE forming simulations. It should be noted that in the simulation, a COF of below or slightly above 0.01 does not significantly change the punch force, which is discussed at the end of this section. This is also indicated by the small variations in the experimental punch force in Figure 11.

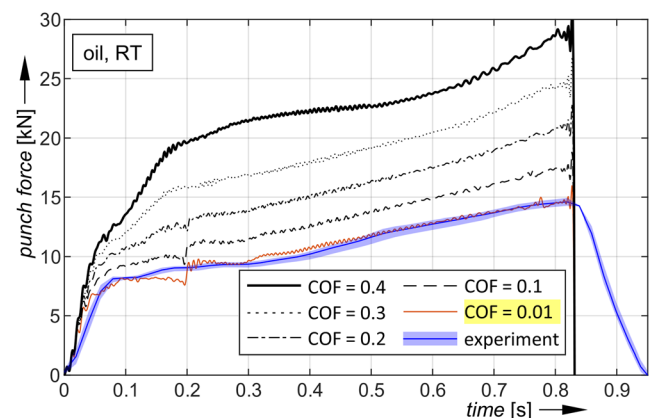


Figure 11. Comparison of experimental and FE punch forces for oil at RT. The highlighted COF curve represents predicted COF from the strip drawing test.

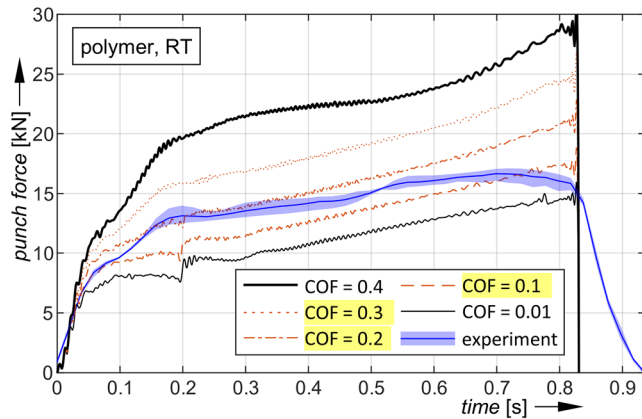


Figure 12. Comparison of experimental and FE punch forces for polymer at RT.

For the polymer at RT, the result of the comparison is not as obvious as for the oil. **Figure 12** shows that the COF of 0.4 obtained in the strip drawing tests at 5 MPa is not reached in the FE analyses. This can be explained by the higher contact pressure peaks at the die radius, which may approximate the targeted working conditions of a bulk metal forming lubricant such as the polymer. Higher contact pressure leads to higher frictional heat and therefore higher contact temperature in the forming process. Figure 5 shows a significant decrease in the COF of the polymer with increasing temperature. The strip drawing tests at 20 MPa lead to a better fit of the COF, which can be explained by both the approximation to the intended working conditions of the lubricant and the higher frictional heat (lower friction) compared to the 5 MPa results. Another observation is the variation of the COF between 0.2 at the beginning of the experimental forming process and 0.1 after about 0.7 s. This behavior can also be explained by an increasing contact temperature (=lower friction) over the forming process. A time stamp for the end of wear-free sliding cannot be conclusively determined from the results in Figure 10 in comparison with the marks in the wall area shown in Figure 7. The slight increase in COF at 0.15 s (Figure 12) may indicate a scraping of the polymer lubricant from parts of the die radius. Previous studies in the strip drawing test show that, especially at room temperature, the polymer lubricant is scraped off the die surface under combined normal and sliding loads.^[22]

The punch force results for the FE-based and experimental studies of BN show good agreement (cf., **Figure 13**). In the strip drawing tests, the BN detached from the die surface in an irregular pattern and also showed a high fluctuation in the wear-free draw in.^[22] An analogous behavior is indicated by the variation of the experimental punch forces between 0.2 and 0.6 s in Figure 13.

The question of why the COFs of 5 and 3 MPa strip drawing tests are suitable for oil and BN, while only the COF of 20 MPa strip drawing tests is suitable for the polymer forming trials, is discussed below. In previous studies, the polymer showed a significant decrease in COF with increasing contact temperature, regardless of whether the contact temperature was increased by using higher temperature sheets or higher temperature dies.^[21] It is assumed that the higher frictional heat induced by the higher contact pressure also decreases the polymer COF. Regarding the contact pressure itself (ignoring any possible

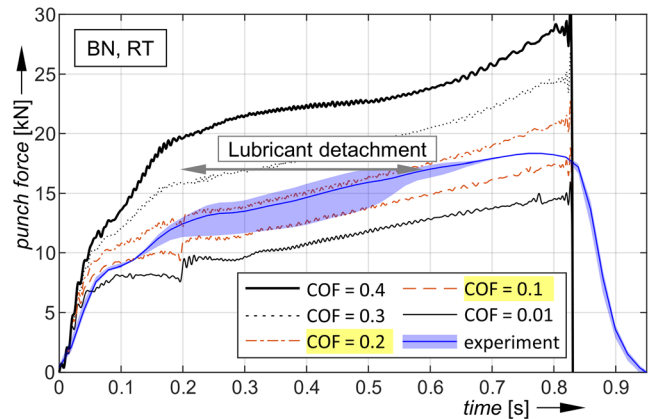


Figure 13. Comparison of experimental and FE punch forces for BN at RT.

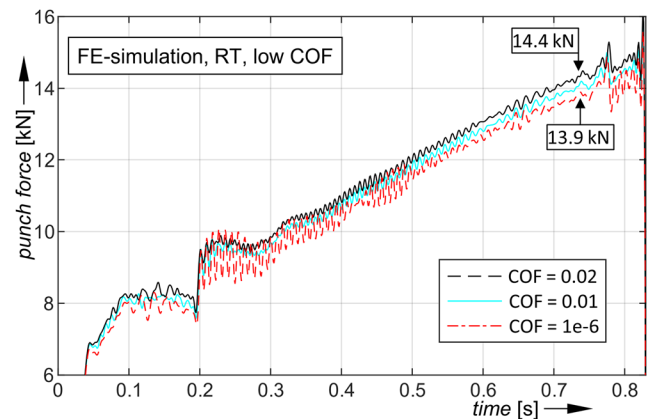


Figure 14. FE punch forces at RT with low COF.

increase in frictional heat), it is known from the literature that for oil lubricants the COF decreases with increasing contact pressure at low to medium^[29] and also at high contact pressure levels.^[30] However, in this article the COF for oil at 3 and 5 MPa is already very low (cf., Figure 5). If strip drawing tests at 20 MPa would result in the same or even lower COF, this would not affect the fit of the FE and experimental punch force curves in Figure 11 because reducing the COF in the FE simulation below 0.01 does not significantly change the punch force (but does increase the solution noise, cf., **Figure 14**). In other words, for the oil, the experimental punch force would also match the COF from 20 MPa strip drawing tests. The same conclusion can be drawn for BN, which has already been investigated in 10 MPa strip drawing tests with no significant change in COF compared to lower contact pressure tests.^[22]

3.3.2. Warm Forming

At warm forming temperature, the experimental punch force for the oil lubricant is at the upper end of the punch force predicted from the FE analyses with the highlighted COF from the strip drawing tests (cf., **Figure 15**). Possible explanations for this are the temperature-dependent modeling of the aluminum's yield stress with uncertainties between RT and 200 °C and

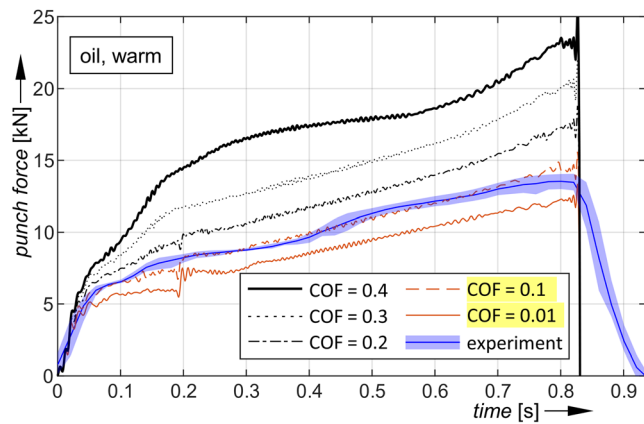


Figure 15. Comparison of experimental and FE punch forces for oil at warm forming temperature.

different contact area sizes between the strip drawing tests (large contact area) and at the die radius (small contact area). An influence of contact size on friction in oil-lubricated strip drawing^[31] and cylinder compression tests^[32] is reported in the literature, where smaller contact sizes lead to higher COFs.

For the BN and the polymer lubricants, the experimental punch forces are in the expected range at the beginning of forming but exceed the corresponding FE punch forces after 0.1 to 0.2 s (cf., **Figure 16**). However, in contrast to the oil lubricant,

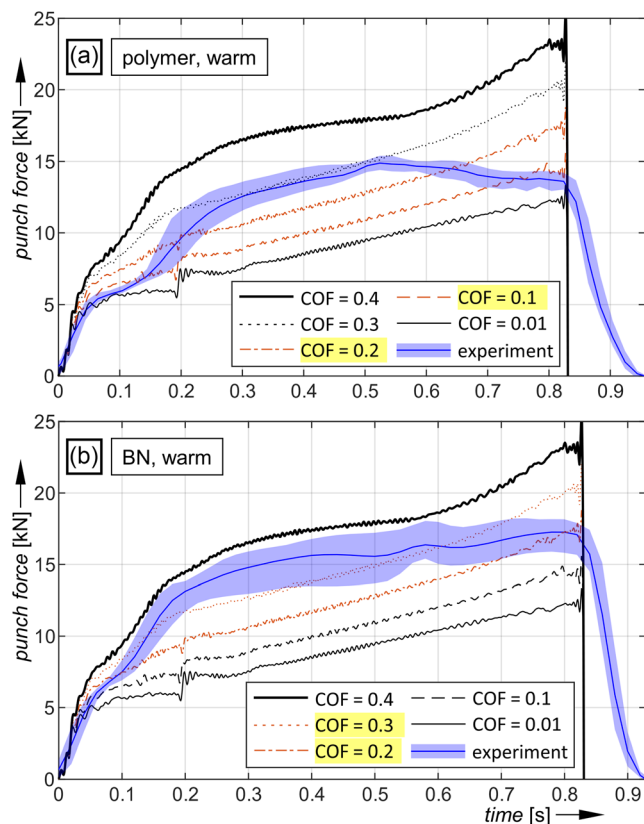


Figure 16. Comparison of experimental and FE punch forces for a) polymer and b) BN at warm forming temperature.

the wear in the BN and polymer forming trials is more severe than in the strip drawing tests, which explains the comparatively higher experimental punch force. As a result, for BN and polymer, a direct comparison between the COFs from the strip drawing test and the COF in the FE/experimental punch force is problematic. To improve this comparability, further lubricant developments are needed to prevent wear in both the strip drawing test and the forming trials (at least within the scope of the comparison). Only if there is no immediate wear in both processes, a deeper discussion of the influence of the contact conditions on the COF and its transferability from the strip drawing test to real forming trials is meaningful.

3.3.3. Hot Forming

For the oil and polymer trials at hot forming temperature, the experimental punch force curves are mostly between the corresponding punch force curves from the FE analyses (cf., **Figure 17**). This indicates a good transferability of the COF results from strip drawing tests to real forming processes.

In the case of BN, the experimental punch force exceeds the expected FE punch force (cf., **Figure 18**). This can be explained by more severe wear at the die radius in the forming process compared to the strip drawing tests. In the strip drawing tests, local damage to the lubricant layer does not necessarily result in direct metal-to-metal contact or increased COF because the surrounding incompressible lubricant particles provide load-bearing

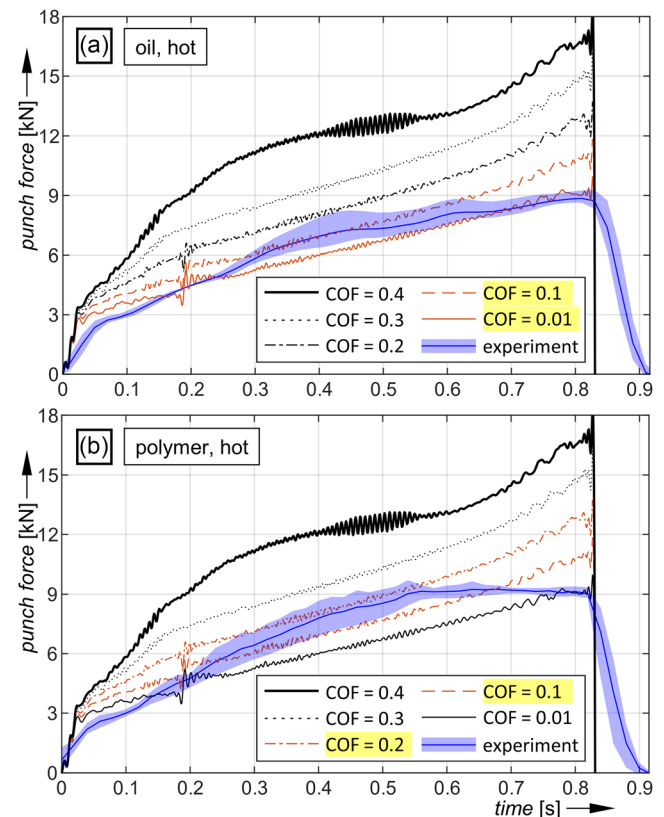


Figure 17. Comparison of experimental and FE punch forces for a) oil and b) polymer at hot forming temperature.

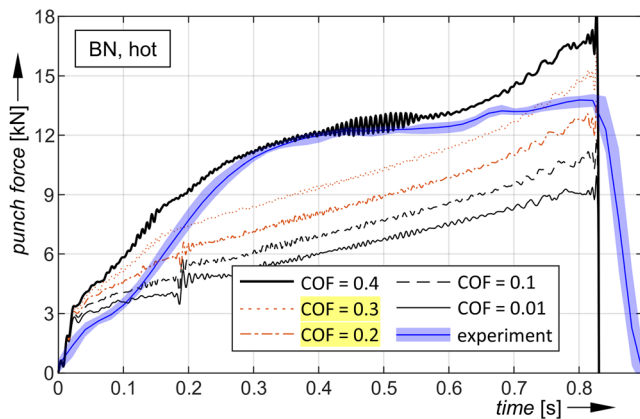


Figure 18. Comparison of experimental and FE punch forces for BN at hot forming temperature.

effect. However, the die radius of the forming process is more prone to local contact pressure peaks,^[33] leading to direct metal-to-metal contact and thus more severe wear and higher COF.

4. Conclusion and Outlook

Knowledge of the transferability of tribological test results to real forming processes is of great importance for process design. In particular, the transferability has not yet been investigated for temperature-supported forming processes of high-strength aluminum sheet. Therefore, the COF has been determined for different temperatures and lubricants in temperature-controlled flat die strip drawing tests.^[22] In the current article, a thermomechanical FE forming analysis of a hat profile geometry was performed with a variation of COFs that represent the COFs from the strip drawing tests.

The punch forces from the FE analyses were compared to the punch forces from forming trials with different lubricants. While in some cases the results show good agreement (e.g., oil at RT and hot forming temperature), other results are difficult to fully evaluate: It was shown that further advances in thermomechanical material modeling are needed, especially to account for non-linear material behavior at temperatures between 200 and 20 °C. In addition, the difference in wear behavior between strip drawing tests and forming trials is an issue, especially under hot forming conditions. For the evaluation of the wear behavior, additional investigations should be carried out with cylinder plane strip drawing tests to better simulate the local contact conditions at the forming die radius.^[33]

Furthermore, it was shown that when unlubricated aluminum blanks are formed in lubricated dies, the lubricant performance may depend significantly on the state of aggregation of the lubricant, or in other words, its ability to transfer from the die to the blank at low contact pressure. Therefore, the contact history and sliding path of the aluminum blank in the die must be considered in the design of forming processes with die lubrication.

In summary, the combination of strip drawing tests, FE forming simulations, and forming trials improves the overall understanding of the challenges in the design of temperature-

supported aluminum sheet metal forming processes. Considering the extensive tribometer developments for room temperature sheet metal forming,^[9] it can be stated that there is still a lot of research to be done in the field of tribological assessment of temperature-supported aluminum forming processes.

Acknowledgements

The analyses in this article were carried out as part of the dual doctorate program of the “PrositAl dual” project in cooperation with FILZEK TRIBOtech. This project (HA project no. 1269/21-170) was financed with funds of LOEWE—Landes-Offensive zur Entwicklung Wissenschaftlich-ökonomischer Exzellenz, Förderlinie 3: KMU-Verbundvorhaben (State Offensive for the Development of Scientific and Economic Excellence).

Open Access funding enabled and organized by Projekt DEAL.

Conflict of Interest

The authors declare no conflict of interest.

Data Availability Statement

Research data are not shared.

Keywords

high-strength aluminum, hot forming, sheet metal forming, strip drawing tests, tribology

Received: December 28, 2022

Revised: March 1, 2023

Published online: April 20, 2023

- [1] J. Mendiguren, E. S. de Argandona, L. Galdos, *IOP Conf. Ser.: Mater. Sci. Eng.* **2016**, 159, 12026.
- [2] G. Anyasodor, C. Koroschetz, *IOP Conf. Ser.: Mater. Sci. Eng.* **2018**, 418, 12023.
- [3] T. Grohmann, *Forming of AMAG 7xxx Series Aluminium Sheet Alloys*, AMAG rolling GmbH, Braunau, Austria **2016**.
- [4] B. Myrold, O. Jensrud, K. E. Snilsberg, *Metals* **2020**, 10, 935.
- [5] K. Zheng, Y. Dong, H. Dong, J. Fernandez, T. A. Dean, *Procedia Eng.* **2017**, 207, 711.
- [6] Y. Liu, Z. Zhu, Z. Wang, B. Zhu, Y. Wang, Y. Zhang, *Procedia Eng.* **2017**, 207, 723.
- [7] M. Merklein, J. Degner, *Fertigung hochfester Aluminiumbauteile durch Umformen unter Abschreckbedingungen*, Europäische Forschungsgesellschaft für Blechverarbeitung e.V, Hannover **2018**.
- [8] T. Trzepieciniski, H. G. Lemu, *Metals* **2020**, 10, 47.
- [9] L. Schell, P. Groche, in *Forming the Future* (Eds: G Daehn, J Cao, B Kinsey, E Tekkaya, A Vivek, Y Yoshida), Springer International Publishing, Cham **2021**, pp. 81–96.
- [10] M. Vilaseca, S. Molas, D. Casellas, *Wear* **2011**, 15, 420.
- [11] M. D. Hanna, in *Part B: Magnetic Storage Tribology; Manufacturing/Metalworking Tribology; Nanotribology; Engineered Surfaces; Biotribology; Emerging Technologies; Special Symposia on Contact Mechanics; Special Symp. Nanotribology*, ASME, San Antonio, TX **2006**, pp. 917–922.
- [12] B. Podgornik, T. Kosec, A. Kocijan, Č. Donik, *Tribol. Int.* **2015**, 81, 267.

- [13] B. Podgornik, F. Kafexhiu, T. Kosec, J. Jerina, M. Kalin, *Wear* **2017**, 388–389, 2.
- [14] M. D. Hanna, P. E. Krajewski, J. G. Schroth, in *ASME/STLE 2007 Int. Joint Tribology Conf., Parts A and B*, ASME, San Diego, CA **2007**, pp. 705–707.
- [15] J. Decrozant-Triquenaux, L. Pelcastre, B. Prakash, J. Hardell, *Friction* **2020**, 9, 155.
- [16] Z. Shi, L. Wang, M. Mohamed, D. S. Balint, J. Lin, M. Stanton, D. Watson, T. A. Dean, *Procedia Eng.* **2017**, 207, 2274.
- [17] F. Medea, A. Ghiotti, S. Bruschi, *Key Eng. Mater.* **2015**, 639, 221.
- [18] A. Ghiotti, S. Bruschi, F. Medea, *Wear* **2017**, 376–377, 484.
- [19] Y. Liu, B. Zhu, K. Wang, S. Li, Y. Zhang, *Tribol. Int.* **2020**, 151, 106504.
- [20] N. Rigas, F. Junker, E. Berendt, M. Merklein, *DDF* **2022**, 414, 125.
- [21] L. Schell, P. Groche, *DDF* **2022**, 414, 95.
- [22] L. Schell, M. Emele, A. Holzbeck, P. Groche, *Tribol. Int.* **2022**, 168, 107449.
- [23] S. V. Sajadifar, E. Scharifi, U. Weidig, K. Steinhoff, T. Niendorf, *Metals* **2020**, 10, 884.
- [24] S. Ekşi, H. Pehlivan, *Mater. Test.* **2022**, 64, 1410.
- [25] H. Wang, Y. Luo, P. Friedman, M. Chen, L. Gao, *Trans. Nonferrous Met. Soc. China* **2012**, 22, 1.
- [26] M. Jäckel, S. Maul, C. Kraus, W.-G. Drossel, *J. Phys.: Conf. Ser.* **2018**, 1063, 12074.
- [27] X. Liu, K. Ji, O. E. Fakir, H. Fang, M. M. Gharbi, L. Wang, *J. Mater. Process. Technol.* **2017**, 247, 158.
- [28] J. Filzek, *Kombinierte Prüfmethode für das Reib-, Verschleiß- und Abriebverhalten beim Tief und Streckziehen*. Jan Filzek. Zugl.: Darmstadt, Technical University, Diss., 2004, Shaker, Aachen **2004**.
- [29] J. Filzek, M. Ludwig, P. Groche, in *Proc. IDDRG*, Bilbao, Spain **2011**, pp. 5–8.
- [30] F. Vollertsen, Z. Hu, *Prod. Eng. Res. Dev.* **2008**, 2, 345.
- [31] V. Recklin, F. Dietrich, P. Groche, *Lubricants* **2018**, 6, 41.
- [32] B. Guo, F. Gong, C. Wang, D. Shan, *Trans. Nonferrous Met. Soc. China* **2009**, 19, s516.
- [33] P. Groche, J. Filzek, G. Nitzsche, *Prod. Eng.* **2004**, 11, 55.
- [34] voestalpine High Performance Metals Deutschland GmbH, *Materialdaten_Unimax*: E-Mail: 22.01.2021, Vol. 12, Thomas Schmidt, Duesseldorf, Germany **2021**, p. 19.
- [35] Z. Guo, H. Zhu, S. Cui, Y. Wang, *Trans. China Weld. Inst.* **2015**, 36, 92.
- [36] UDDEHOLMS AB, *UDDEHOLM UNIMAX: Data Sheet. Classified According To EU Directive 1999/45/EC*, 6th ed., Hagfors, Sweden **2015**.